

Contents

1. SEISMIC HAZARD ASSESSMENT OF LLOGARA TUNNEL SITE (VLORA DISTRICT)	4
1.1 Introduction	4
1.2 Probabilistic seismic hazard assessment	5
1.2.1 Source modelling and assumptions	5
1.2.2 Hazard curves	7
1.2.3 Uniform Hazard Spectrum	9
1.2.4 Disaggregation analysis	10
1.3 Deterministic seismic hazard assessment	11
1.4 Assessment of Duration of Strong Earthquake Shaking at Building Site	13
1.5 Topographic amplification according to EC8 Part 5	14
1.6 Elastic spectra according to EC8 and Acceleration time histories	16
1.6.1 Design Spectrum based on EC8	16
1.6.2 Vertical Elastic Spectra	18
1.6.3 Ground Motion Time Histories compatible with EC8 Part 2 requirements	19
1.6.4 Selected records and discussion	19
1.7 Analysis of the actual in force Albanian design code in respect to seismic action and comparisons with the requirements of EC8.	24
1.8 Conclusion and Recommendations	26
1.9 Deliverables	27
1.10 References	27

List of Figures:

Figure 1.1 Representative locations of the construction works and nearby seismogenic faults. Source: OSM and EDSF ..	4
Figure 1.2 Spatial distribution of the earthquake epicenters in the study region (510 B.C.–31/12/2008, $M_w \geq 4.0$), and the seismo-tectonic zones used for seismic hazard assessment.....	5
Figure 1.3 Delineation of the considered are source zones adopted from Muco et al. (2002)	6
Figure 1.4 Hazard curves for multiple intensity measures considered in this study.....	7
Figure 1.5 Uniform hazard Spectra using (non-logarithmic)	9
Figure 1.6 Uniform hazard Spectra (Logarithmic).....	9
Figure 1.7 Disaggregation analysis results	10
Figure 1.8 Location of the closest faults to the site of interest.	11
Figure 1.9 Comparison between the scenario-based response spectra (mean $\pm 1\sigma$) for two deterministic scenarios using the Akkar et al. (2014) GMPE.....	13
Figure 1.10 Comparison between the scenario-based mean response spectra for two deterministic scenarios using different GMPEs.	13
Figure 1.11 Suggested values for the topographic amplification factor S_T in Eurocode 8 Part 5 (adapted from Pagliaroli et al. 2007).....	14
Figure 1.12 Plan view of the broad site area and the location of the cross sections, source: Google Earth.....	15
Figure 1.13 Cross-sections in the positions 1-1, 2-2, 3-3 and the average angle of the sea-side slopes.....	15
Figure 1.14 UHS and EC8-Type 1 spectra for different return periods.....	17
Figure 1.15 UHS and EC8-Type 2 spectra for different return periods.....	18
Figure 1.16 Horizontal ground motion records selected corresponding with the EC8-Type 1 design spectrum.....	21
Figure 1.17 Vertical ground motion records selected corresponding with the EC8-Type 1 design spectrum	22
Figure 1.18 Horizontal ground motion records selected corresponding with the EC8-Type 2 design spectrum.....	22
Figure 1.19 Vertical ground motion records selected corresponding with the EC8-Type 2 design spectrum	23
Figure 1.20 Seismic hazard map in KTP-N2-89, in MSK-64 macroseismic intensity scale	24
Figure 1.21 Comparison of the horizontal elastic spectra according to KTP N.2 89 and EC8.....	26
Figure 1.22 Comparison of the vertical elastic spectra according to KTP N.2 89 and EC8	26

List of Tables:

Table 1.1 Gutenberg-Richter Recurrence parameters, estimated by Maximum Likelihood Method adopted from Muco et al. (2002)	6
Table 1.2 Seismic hazard curves for different spectral ordinates	8
Table 1.3 Uniform hazard spectra [g] for different return periods	10
Table 1.4 Features of the two closest faults to the site of interest	11
Table 1.5 Response spectra for the selected deterministic scenario of M7.2, R8.2 (Fault name: Sazani)	11
Table 1.6 Response spectra for the selected deterministic scenario of M6.0, R4.2 (Fault name: Vlora)	12
Table 1.7. Median and standard deviation of the duration (DS_{5-95}) in seconds for the selected likely scenarios of the site of interest.	13
Table 1.8 Recommended values of parameters describing the horizontal elastic response spectra (EC8)	16
Table 1.9: Reference ground acceleration computed from the PSHA analysis presented in Chapter 4	17
Table 1.10 Recommended values of parameters describing the vertical elastic response spectra (excerpt from EC8)	18
Table 1.11 Horizontal ground motion records selected corresponding with the EC8-Type 1 design spectrum	20
Table 1.12 Vertical ground motion records selected corresponding with the EC8-Type 1 design spectrum	20
Table 1.13 Horizontal ground motion records selected corresponding with the EC8-Type 2 design spectrum	20
Table 1.14 Vertical ground motion records selected corresponding with the EC8-Type 2 design spectrum	21
Table 1.15 Seismic coefficients according to KTP-N.2-89	25
Table 1.16: Dynamic factor β , according to KTP-N.2-89	25
Table 1.17 Table of deliverables of this study	27

1. SEISMIC HAZARD ASSESSMENT OF LLOGARA TUNNEL SITE (VLORA DISTRICT)

1.1 Introduction

On a hilly-mountainous terrain in Albania's southwest, the tunnel site area is situated in one of Albania's most seismoactive region, the Ionian-Adriatic seismogenic belt, that is responsible for generating numerous strong damaging earthquakes as reported by Aliaj et al. 2010. The area is hit periodically by strong earthquakes with the highest recorded surface magnitudes, M_s , of 6.6. The last damaging earthquake in the region that caused 30 fatalities is recorded in 1930. According to Aliaj et al. 2010, the shaking destroyed several nearby villages and was estimated with a seismic intensity IX according to the MSK 64 scale (Medvedev et al. 1964). The tunnel area is located between at least two well-known active faults, Figure 1.1, with one of them having the capacity to generate earthquakes with moment magnitudes, M_w , up to 7.2 according to the European Database of Seismogenic Faults (EDSF) (Basili et al. 2013).

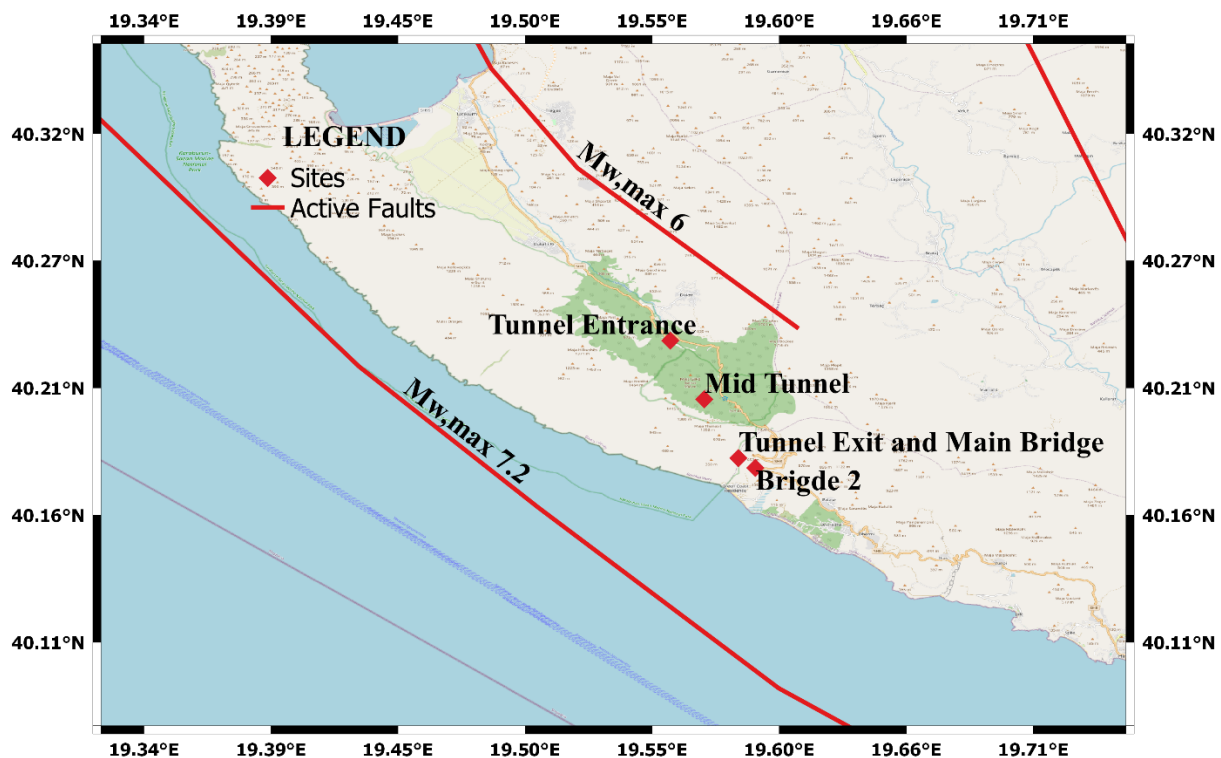


Figure 1.1 Representative locations of the construction works and nearby seismogenic faults.
 Source: OSM and EDSF

This chapter's broad scope is to present the results of the probabilistic and deterministic seismic hazard assessment (PSHA and DSHA) analyses of the tunnel site area. We have done an extensive review of the current PSHA models of Albania and have decided to select the model from Duni et al. 2010. The provided outputs of the PSHA are the Uniform Hazard Spectra (UHS) for four different return periods, the hazard curves for various spectral accelerations, and the 3D plots of disaggregation results. We provide the deterministic response spectra at three different reliability levels, at the median and median \pm sigma level, using three different ground motion prediction equations (GMPEs). Subsequently, we describe the elastic response spectra in line with Eurocode 8 (EC 8) requirements and provide an evaluation of the topographic amplification factor, S_T . We use the EC 8 Part 2 requirements to construct the target response spectra for the ground motion selections. Two sets of seven 3D real ground acceleration time histories are provided. We describe the seismic hazard demand in the tunnel site area according to the Albanian Seismic Design Code, KTP N.2-89. Besides, a

comparison between the KTP N.2-89 and EC8 seismic demand is carried out. Finally, a description of the deliverables is presented at the end of the report.

1.2 Probabilistic seismic hazard assessment

1.2.1 Source modelling and assumptions

Herein, a probabilistic seismic hazard model developed for Albania (Duni et al. 2010) is used for seismic hazard assessment of the interested site. This model was generated in the framework of NATO SfP 983054 project "Harmonization of Seismic Hazard Maps for the Western Balkan Countries" funded by Science for Peace and Security Programme of NATO. The hazard model is generated based on extensive research and database. It uses a uniform (based on moment magnitude) catalog by aggregating the historical and the instrumental earthquake catalogs within the region. The catalog contains events with magnitude $M_s \geq 4.5$ and it covers the time period of 58 BC up to 31/12/2008, and the area between 18.5-21.5°E and 39-43°N. In estimation of the earthquake recurrence parameters, the data completeness in time and space is also controlled and the catalog is de-clustered to remove the foreshocks and aftershocks. The catalog of the events is shown in Figure 1.2.

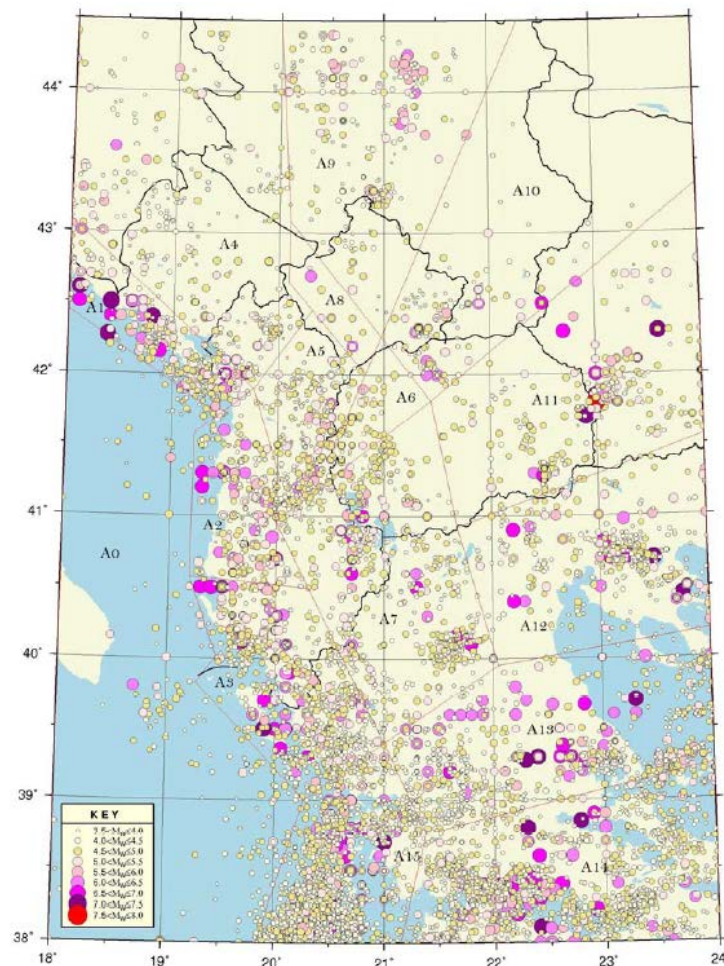


Figure 1.2 Spatial distribution of the earthquake epicenters in the study region (510 B.C.–31/12/2008, $M_w \geq 4.0$), and the seismo-tectonic zones used for seismic hazard assessment.

The seismic sources are characterized based on area sources assuming uniform seismicity within each polygon. As such, 16 seismic zones, namely A0 to A15, are delineated to represent the spatial variation of the seismicity in space. Figure 1.3 shows the extent of the polygons on the map while the location of the interested site is also shown by star symbol. The zone delineation was performed taking into account multiple aspects such as similarity of the geodynamic behavior and the homogeneity of the spatial earthquake epicenter distribution. Accordingly, for each area source polygon, the magnitude-frequency relation coefficients (a - and

b -values in G-R relation), the mean annual rate of seismic activity, the minimum magnitude (M_{min}) and the maximum magnitude (M_{max}) expected to occur within each polygon are estimated. Seismic activity rate is estimated using the double truncated exponential recurrence relationship while the authors evaluated the recurrence parameters using the maximum likelihood approach (MLE) based on multiple approaches. Note that the differences among approaches was shown negligible and therefore, herein use only the results obtained from Weichert (1980) is used. The final recurrence parameters used herein are listed in Table 1.1. M_{max} was estimated using the approach of Kijko (2004) and the previous estimates based on geological consideration.

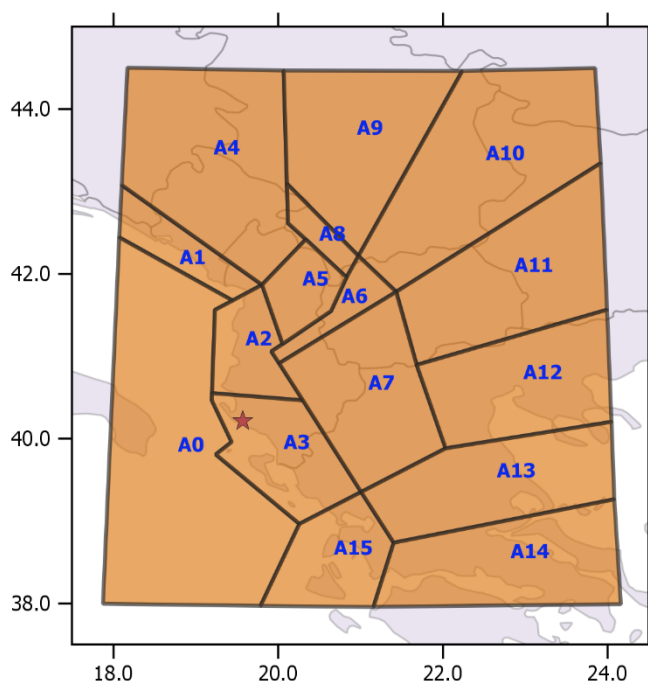


Figure 1.3 Delineation of the considered area source zones adopted from Duni et al. 2010

Table 1.1 Gutenberg-Richter Recurrence parameters, estimated by Maximum Likelihood Method adopted from Duni et al. 2010

Zone	No. Events	M_{obs}	a Value	b Value	M_{max}
A0	43	6.0	7.129	1.628	6.1
A1	57	7.2	3.889	0.918	7.3
A2	77	6.8	4.599	1.031	6.9
A3	247	7.0	5.592	1.133	7.0
A4	60	5.7	4.98	1.127	6.0
A5	37	6.1	5.329	1.277	6.5
A6	41	6.2	5.135	1.201	6.6
A7	133	6.7	5.857	1.247	6.8
A8	7	6.0	4.185	1.161	6.3
A9	45	5.9	4.400	1.032	6.1
A10	24	6.5	4.052	1.021	6.7
A11	85	7.7	5.795	1.277	7.7
A12	93	7.0	6.101	1.333	7.2

A13	141	7.0	5.432	1.153	7.2
A14	272	7.0	6.256	1.267	7.2
A15	247	7.4	5.477	1.119	7.4

The OpenQuake engine (Pagani et al. 2014) for modeling the area sources and for all the hazard computations of this study is adopted. Following suggestions of Mihaljević et al. (2017), the area source are modeled with upper and lower seismogenic sources of 0 and 20 km and a hypo-central depth of [8, 12, 16] km with the weights of [0.25, 0.5, 0.25]. To estimate the rake, DIP and strike angles within each polygon, the European Database of Seismogenic Faults (Basili et al. 2013) is considered to compute the distribution of these angles and assigned to each polygon. In addition, as per suggestions of Gulerce et al. (2017) four ground motion prediction equations (GMPEs) are considered in a GMPE logic tree using Akkar et al. (2014), Bindi et al. (2014), Chiou and Youngs (2014) and Boore et al. (2014) with the weights of 0.2, 0.2, 0.3 and 0.3, respectively.

1.2.2 Hazard curves

PSHA is performed for multiple spectral ordinates including PGA and spectral accelerations (SA) at $T = 0.1s, 0.2s, 0.3s, 0.5s, 0.75s, 1.0s, 1.5s, 2.0s, 3.0s$ and $4.0s$. Four sites located at [19.558258°E, 40.232303°N], [19.572348°E, 40.208022°N], [19.586438°E, 40.183741°N] and [19.593467°E, 40.179692°N] are considered in the computations and the site that provides the most conservative values is suggested for the design purposes. Figure 3 show the hazard curve of all intensity measures while the values are tabulated in Table 1.2.

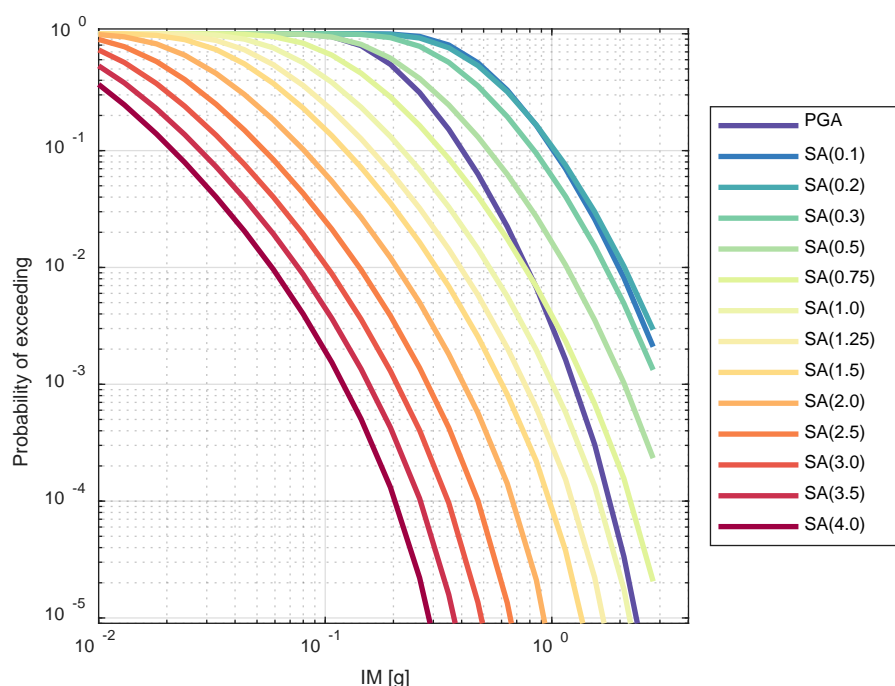


Figure 1.4 Hazard curves for multiple intensity measures considered in this study

Table 1.2 Seismic hazard curves for different spectral ordinates

IM value [g]	PGA	SA(0.1)	SA(0.2)	SA(0.3)	SA(0.5)	SA(0.75)	SA(1.0)	SA(1.25)	SA(1.5)	SA(2.0)	SA(2.5)	SA(3.0)	SA(3.5)	SA(4.0)
0.01	1.00E+00	1.00E+00	1.00E+00	1.00E+00	1.00E+00	1.00E+00	1.00E+00	1.00E+00	1.00E+00	9.84E-01	8.95E-01	7.28E-01	5.32E-01	3.69E-01
0.013	1.00E+00	1.00E+00	1.00E+00	1.00E+00	1.00E+00	1.00E+00	1.00E+00	1.00E+00	9.96E-01	9.41E-01	7.75E-01	5.67E-01	3.79E-01	2.46E-01
0.018	1.00E+00	1.00E+00	1.00E+00	1.00E+00	1.00E+00	1.00E+00	1.00E+00	9.95E-01	9.68E-01	8.20E-01	5.79E-01	3.75E-01	2.29E-01	1.39E-01
0.024	1.00E+00	1.00E+00	1.00E+00	1.00E+00	1.00E+00	1.00E+00	9.97E-01	9.68E-01	8.91E-01	6.56E-01	4.06E-01	2.40E-01	1.37E-01	7.92E-02
0.033	1.00E+00	1.00E+00	1.00E+00	1.00E+00	1.00E+00	9.99E-01	9.73E-01	8.78E-01	7.33E-01	4.58E-01	2.49E-01	1.35E-01	7.28E-02	4.01E-02
0.044	1.00E+00	1.00E+00	1.00E+00	1.00E+00	1.00E+00	9.90E-01	9.00E-01	7.30E-01	5.53E-01	3.02E-01	1.50E-01	7.62E-02	3.89E-02	2.05E-02
0.059	1.00E+00	1.00E+00	1.00E+00	1.00E+00	9.99E-01	9.46E-01	7.58E-01	5.44E-01	3.76E-01	1.84E-01	8.38E-02	4.01E-02	1.94E-02	9.64E-03
0.08	9.94E-01	1.00E+00	1.00E+00	1.00E+00	9.88E-01	8.31E-01	5.65E-01	3.61E-01	2.31E-01	1.02E-01	4.30E-02	1.92E-02	8.70E-03	3.98E-03
0.107	9.46E-01	1.00E+00	1.00E+00	9.99E-01	9.38E-01	6.57E-01	3.84E-01	2.23E-01	1.34E-01	5.46E-02	2.12E-02	8.84E-03	3.66E-03	1.54E-03
0.144	7.91E-01	1.00E+00	9.99E-01	9.87E-01	8.12E-01	4.60E-01	2.35E-01	1.26E-01	7.19E-02	2.68E-02	9.55E-03	3.60E-03	1.35E-03	5.03E-04
0.194	5.47E-01	9.95E-01	9.87E-01	9.27E-01	6.19E-01	2.88E-01	1.32E-01	6.61E-02	3.57E-02	1.21E-02	3.85E-03	1.30E-03	4.26E-04	1.31E-04
0.261	3.14E-01	9.49E-01	9.20E-01	7.81E-01	4.14E-01	1.64E-01	6.86E-02	3.21E-02	1.64E-02	5.00E-03	1.38E-03	4.03E-04	1.05E-04	2.20E-05
0.351	1.52E-01	8.02E-01	7.59E-01	5.69E-01	2.46E-01	8.53E-02	3.29E-02	1.43E-02	6.88E-03	1.81E-03	4.25E-04	9.64E-05	1.58E-05	1.83E-06
0.472	6.30E-02	5.65E-01	5.34E-01	3.58E-01	1.31E-01	4.07E-02	1.44E-02	5.81E-03	2.56E-03	5.69E-04	1.01E-04	1.36E-05	1.22E-06	1.35E-08
0.636	2.24E-02	3.30E-01	3.19E-01	1.95E-01	6.27E-02	1.76E-02	5.65E-03	2.05E-03	8.18E-04	1.41E-04	1.34E-05	9.24E-07	0.00E+00	0.00E+00
0.855	6.72E-03	1.64E-01	1.65E-01	9.47E-02	2.72E-02	6.84E-03	1.96E-03	6.27E-04	2.19E-04	2.11E-05	7.89E-07	0.00E+00	0.00E+00	0.00E+00
1.15	1.62E-03	7.00E-02	7.51E-02	4.06E-02	1.05E-02	2.34E-03	5.75E-04	1.54E-04	3.77E-05	1.10E-06	0.00E+00	0.00E+00	0.00E+00	0.00E+00
1.547	3.04E-04	2.58E-02	2.99E-02	1.52E-02	3.54E-03	6.77E-04	1.34E-04	2.21E-05	3.33E-06	0.00E+00	0.00E+00	0.00E+00	0.00E+00	0.00E+00
2.081	3.35E-05	8.15E-03	1.02E-02	4.91E-03	1.03E-03	1.56E-04	1.76E-05	1.33E-06	6.34E-08	0.00E+00	0.00E+00	0.00E+00	0.00E+00	0.00E+00
2.8	1.93E-06	2.10E-03	2.93E-03	1.33E-03	2.33E-04	2.06E-05	9.08E-07	0.00E+00	0.00E+00	0.00E+00	0.00E+00	0.00E+00	0.00E+00	0.00E+00

1.2.3 Uniform Hazard Spectrum

Figure 1.5(normal) and Figure 1.6(log-log) show the horizontal uniform hazard response spectra (UHS) for the 5% damped ratio for the sites located at rock condition for 95, 475, 2475, and 10000-years return periods.

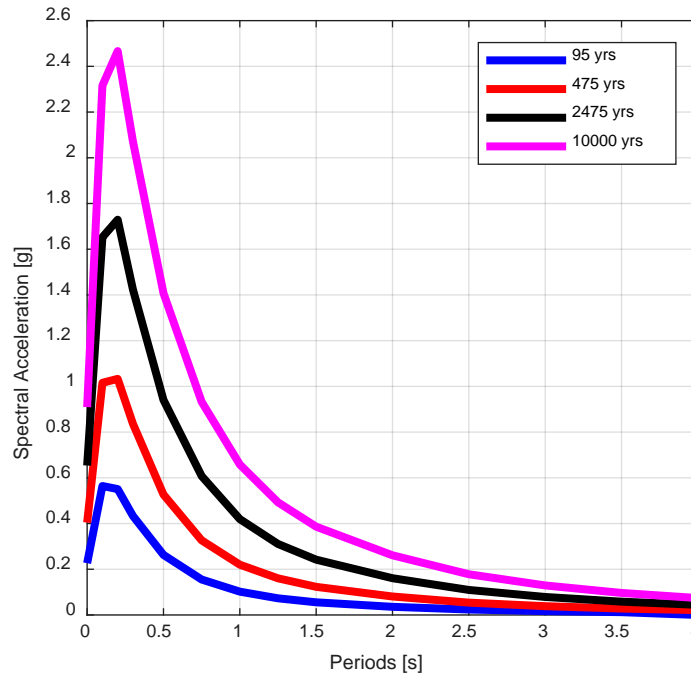


Figure 1.5 Uniform hazard Spectra using (non-logarithmic)

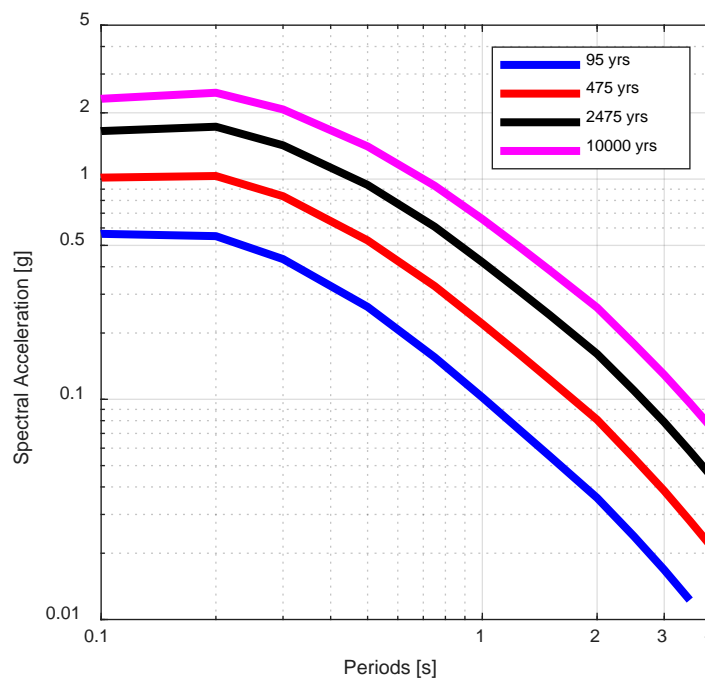


Figure 1.6 Uniform hazard Spectra (Logarithmic)

Table 1.3 Uniform hazard spectra [g] for different return periods

Periods [s]	95 years	475 years	2475 years	10000 years
0.00	0.23	0.40	0.65	0.91
0.10	0.56	1.02	1.65	2.32
0.20	0.55	1.03	1.73	2.47
0.30	0.43	0.84	1.42	2.07
0.50	0.26	0.53	0.94	1.41
0.75	0.16	0.33	0.61	0.93
1.00	0.10	0.22	0.42	0.66
1.25	0.07	0.16	0.31	0.49
1.50	0.06	0.12	0.24	0.39
2.00	0.04	0.08	0.16	0.26
2.50	0.02	0.05	0.11	0.18
3.00	0.02	0.04	0.08	0.13
3.50	0.01	0.03	0.06	0.10
4.00	0.00	0.02	0.04	0.07

1.2.4 Disaggregation analysis

Probabilistic seismic hazard disaggregation analysis is performed for PGA at 475 and 2475 years. The results are shown in Figure 1.7. In this Figure the contribution to hazard for different scenario bins in terms of magnitude, distance and epsilon is shown. Note that epsilon represents the number of standard deviations from the mean (Baker and Cornell 2006). According to these results the most contributions are from $M_w=[5.0, 6.0]$ that happens in a distance of 15-30 km from the site. Still, we argue that because in this study, the area sources are used for seismic hazard modeling, the disaggregation analysis could be significantly affected by this assumption as the seismicity is distributed uniformly all over the area of an area source zone and thus the location of the ruptures may not be a clear representation of real fault ruptures.

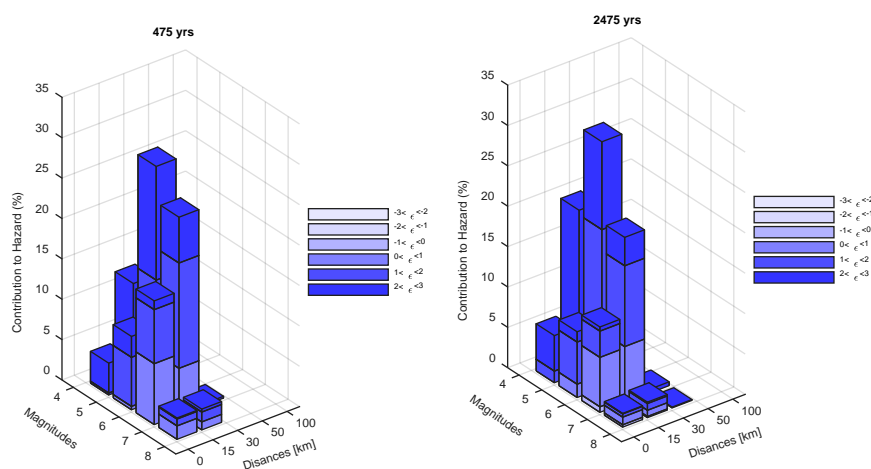


Figure 1.7 Disaggregation analysis results

1.3 Deterministic seismic hazard assessment

The deterministic seismic hazard assessment provides an insight about the impact of the maximum possible earthquake on the site of interest. Herein, the closest identified faults and the maximum possible magnitude along the fault are considered for the deterministic analysis. Figure 1.8 shows the location of the closest site namely Sazani and Vlora according the European Database of Seismogenic Faults (Basili et al. 2013) adopted in this study. The main features of these two faults are listed in Table 2. The maximum magnitude for Sazani and Vlora are M7.2 and M6.0 while closest epicentral distance from the site are 8.2 km and 4.2 km, respectively.

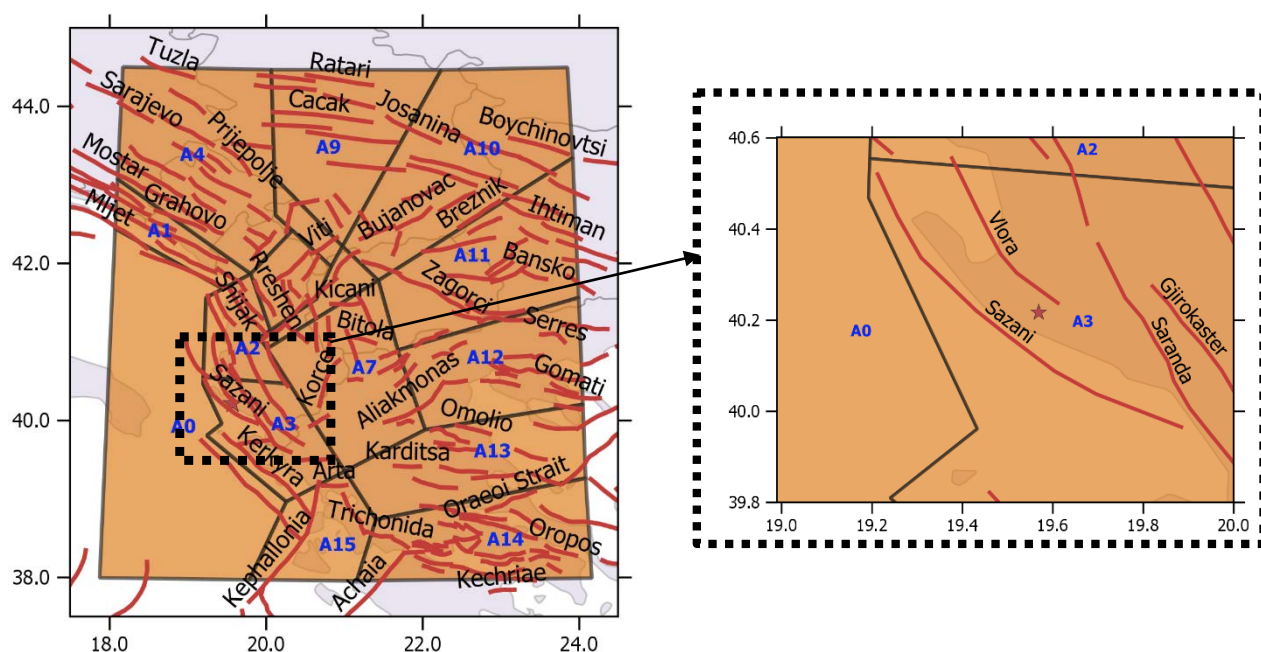


Figure 1.8 Location of the closest faults to the site of interest.

Table 1.4 Features of the two closest faults to the site of interest

Fault Name	Minimum Depth (km)	Maximum Depth (km)	Minimum Dip (°)	Maximum Dip (°)	Minimum Rake (°)	Maximum Rake (°)	Maximum Magnitude (M_B)	Closest Epicentral Distance from Site (km)
Sazani	1	15	25	40	80	100	7.2	8.2
Vlora	1	10	30	45	80	100	6.0	4.2

As such, based on the geometries of the site, two likely scenarios of [M7.2, R8.2] and [M6.0, R4.2] are selected for the deterministic seismic hazard analysis. Figure 1.9 compares the median \pm one standard deviations for both scenarios using the Akkar et al. (2014) GMPE. Figure 1.10 shows and compares the mean response spectra using different GMPEs also adopted in the PSHA study. The results are also tabulated in Table 1.5 and Table 1.6.

Table 1.5 Response spectra for the selected deterministic scenario of M7.2, R8.2 (Fault name: Sazani)

Period [s]	Akkar et al. (2014)		Boore et al. (2014)		Chiou & Youngs (2014)		Equally weighted Average	
	Mean [g]	σ [g]	Mean [g]	σ [g]	Mean [g]	σ [g]	Mean [g]	σ [g]
0.00	0.41	0.32	0.32	0.23	0.45	0.32	0.39	0.29
0.10	0.89	0.73	0.70	0.54	1.05	0.77	0.88	0.73
0.15	0.96	0.79	0.76	0.57	1.12	0.83	0.95	0.77

0.20	0.86	0.70	0.73	0.54	1.09	0.81	0.90	0.71
0.25	0.79	0.64	0.69	0.50	1.02	0.76	0.83	0.66
0.75	0.33	0.27	0.36	0.27	0.51	0.39	0.40	0.35
1.25	0.19	0.16	0.25	0.20	0.31	0.24	0.25	0.23
1.75	0.13	0.11	0.18	0.14	0.23	0.18	0.18	0.17
2.25	0.10	0.08	0.14	0.11	0.17	0.13	0.14	0.13
2.75	0.07	0.06	0.12	0.09	0.13	0.10	0.11	0.10
3.25	0.06	0.05	0.10	0.08	0.10	0.08	0.09	0.08
3.75	0.05	0.04	0.09	0.07	0.08	0.06	0.07	0.07
3.99	0.04	0.03	0.09	0.07	0.07	0.05	0.07	0.06

Table 1.6 Response spectra for the selected deterministic scenario of M6.0, R4.2 (Fault name: Vlora)

Period [s]	Akkar et al. (2014)		Boore et al. (2014)		Chiou & Youngs (2014)		Equally weighted Average	
	Mean [g]	σ [g]	Mean[g]	σ [g]	Mean [g]	σ [g]	Mean [g]	σ [g]
0.00	0.32	0.26	0.35	0.23	0.29	0.20	0.32	0.23
0.10	0.77	0.71	0.84	0.66	0.69	0.53	0.76	0.64
0.15	0.77	0.71	0.92	0.67	0.73	0.58	0.81	0.67
0.20	0.64	0.57	0.86	0.59	0.70	0.56	0.74	0.61
0.25	0.55	0.49	0.74	0.49	0.65	0.53	0.65	0.53
0.75	0.15	0.14	0.26	0.20	0.29	0.25	0.23	0.22
1.25	0.07	0.07	0.15	0.12	0.16	0.13	0.13	0.13
1.75	0.04	0.04	0.09	0.07	0.11	0.09	0.08	0.08
2.25	0.03	0.03	0.06	0.05	0.08	0.06	0.06	0.06
2.75	0.02	0.02	0.04	0.04	0.05	0.04	0.04	0.04
3.25	0.02	0.01	0.04	0.03	0.04	0.03	0.03	0.03
3.75	0.01	0.01	0.03	0.02	0.03	0.02	0.02	0.02
3.99	0.01	0.01	0.03	0.02	0.03	0.02	0.02	0.02

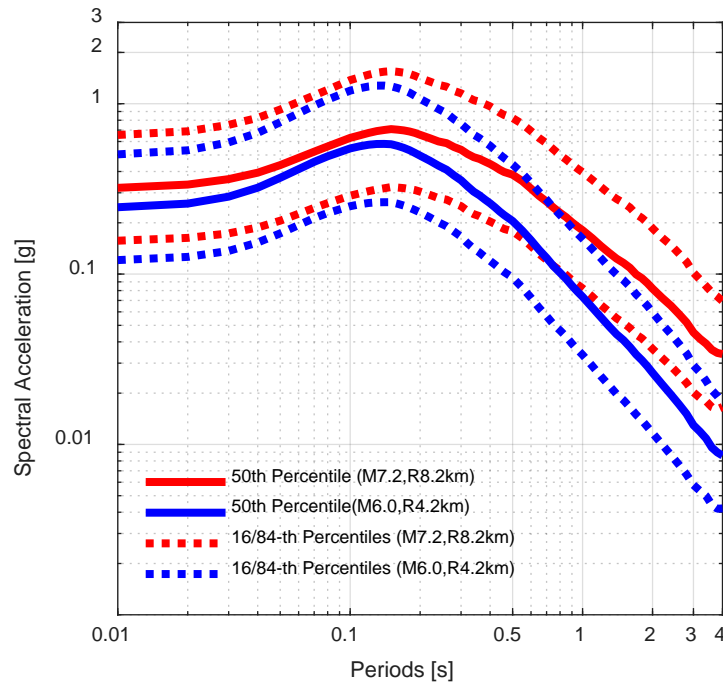


Figure 1.9 Comparison between the scenario-based response spectra 16th/50th/84th percentiles for two deterministic scenarios using the Akkar et al. (2014) GMPE.

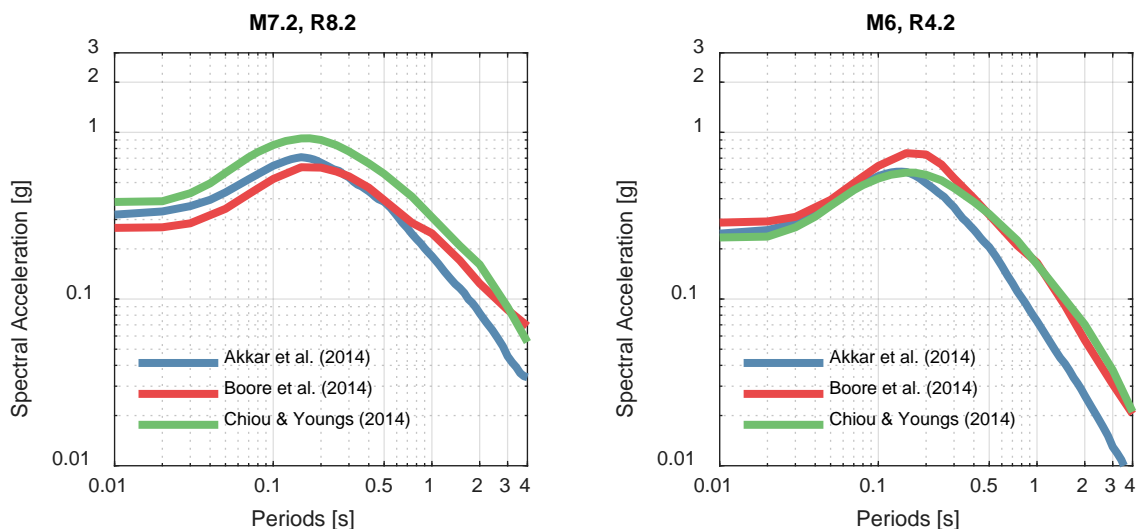


Figure 1.10 Comparison between the scenario-based median (50th Percentile) response spectra for two deterministic scenarios using different GMPEs.

1.4 Assessment of Duration of Strong Earthquake Shaking at Building Site

The duration of the strong ground motions is herein evaluated using the GMPE developed by Afshari and Stewart (2016). Here, the duration is defined as D_{S5-95} . To account for a range of possible distance and magnitudes, twelve possible combinations of $M_w = [5.0, 6.0, 7.0]$ and distances $R = [5, 10, 25, 50]$ km are considered to calculate the median and standard deviation of D_{S5-95} .

Table 1.7. Median and standard deviation of the duration (D_{S5-95}) in seconds for the selected likely

scenarios of the site of interest.

		Median			Logarithmic Standard Deviation ($\sigma_{\text{Ln}(D_{5-95})}$)		
		Magnitude					
		5.0	6.0	7.0	5.0	6.0	7.0
Distance [km]	5	2.7	4.1	7.6	0.50	0.43	0.40
	10	4.1	5.4	8.9	0.50	0.43	0.40
	25	7.4	8.7	12.2	0.50	0.43	0.40
	50	12.8	14.1	17.6	0.50	0.43	0.40

1.5 Topographic amplification according to EC8 Part 5

Since the relief where the site is located is not flat, we need to consider the amplification of earthquake accelerations due to the terrain's geometry. The topographic amplification factor, S_T , is computed based on the requirements of Annex A of Eurocode 8 Part 5. The suggested values of S_T are reported Figure 1.11 for some typical topographic features (slopes, isolated cliffs, and ridges) having an average slope angle $\beta \geq 15^\circ$. Regarding the spatial variation of S_T , the highest values apply near the top of the slopes, while the amplification factor can be assumed to decrease linearly towards the base, where it becomes unity.

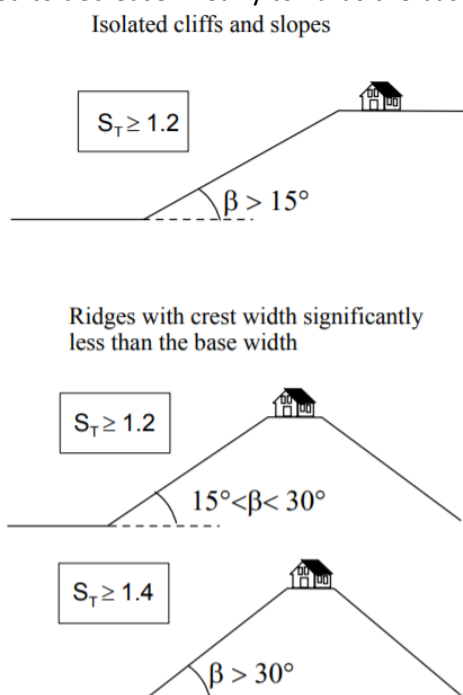


Figure 1.11 Suggested values for the topographic amplification factor S_T in Eurocode 8 Part 5 (adapted from Pagliaroli et al. 2007)

To compute the topographic factors, the slope of the terrain in several cross-sections is calculated, Figure 1.12, Figure 1.13. Since the topographic amplification factor varies linearly from the ridge base where it takes a value equal to 1 up to the ridge crest where it takes its maximal value, as the representative point of the site is considered the entrance of the tunnel, the highest point, with an approximate height of 433m. Considering that the average slope angle is less than 30° , which means that $S_{T,max}$ equals 1.2, the relative height for the ridge base is $\approx 433m/1391m=0.31$, and by rounding the value, we find that the S_T of our construction site is 1.1.

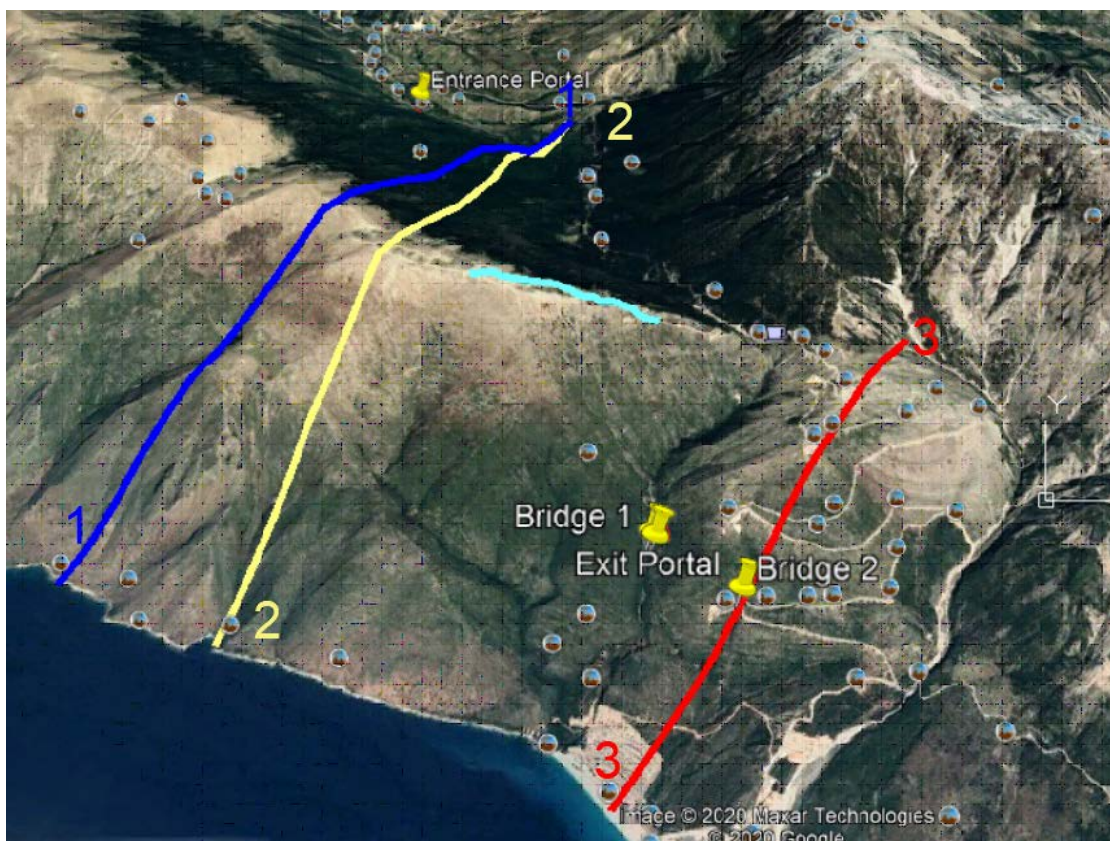


Figure 1.12 Plan view of the broad site area and the location of the cross sections, source: Google Earth

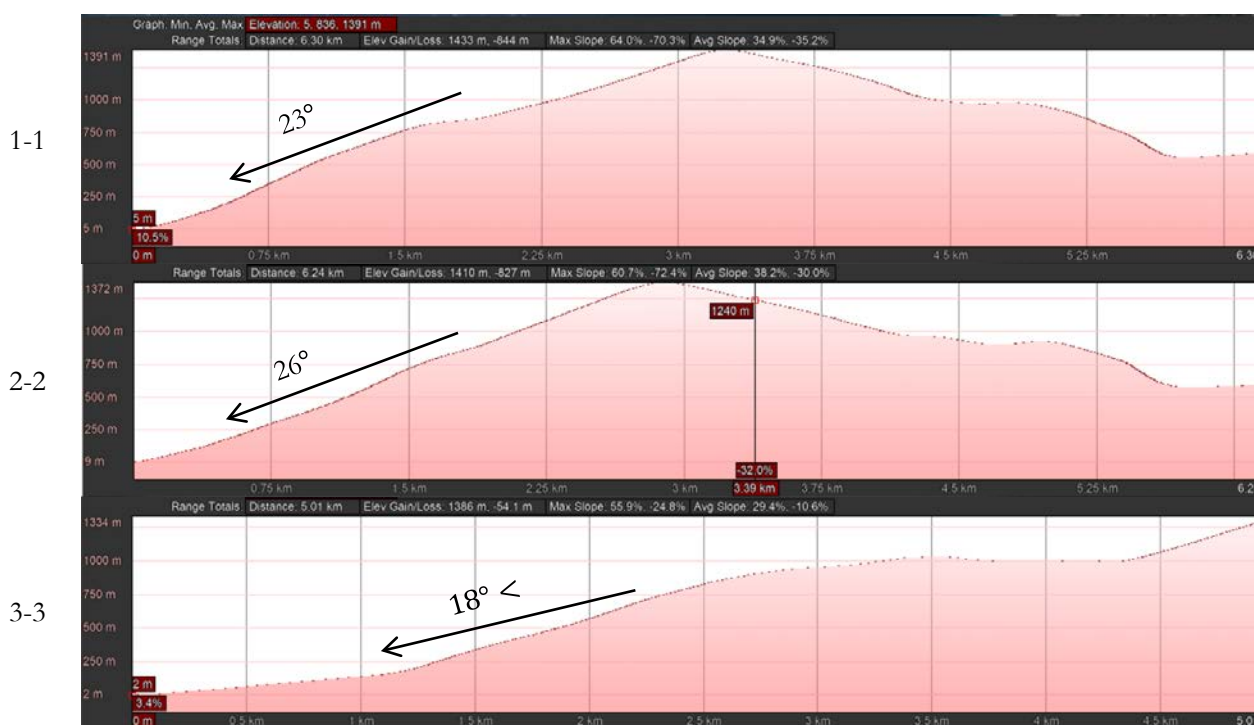


Figure 1.13 Cross-sections in the positions 1-1, 2-2, 3-3 and the average angle of the sea-side slopes

1.6 Elastic spectra according to EC8 and Acceleration time histories

In this section the parameters for creating vertical and horizontal elastic spectra according to the EC8 and the ground motion record selection procedure are described. In the following sub-sections, first the generation of the elastic design spectrum for horizontal and vertical ground shakings based on the Eurocode 8 is described. Subsequently, the record selection criteria according to EC2 are listed and the selected motions are presented.

1.6.1 Design Spectrum based on EC8

For most of the application of EC8 the seismic hazard is expressed in terms of a single parameter, *i.e.*, the value of the reference peak ground acceleration on type A ground, a_{gr} , which can be computed by the PSHA approach. The horizontal elastic spectra according to Eurocode 8 are defined based on the following expressions:

$$0 \leq T \leq T_B: \quad S_e(T) = a_g \cdot S_T \cdot S \cdot \left[1 + \frac{T}{T_B} \cdot (\eta \cdot 2.5 - 1) \right] \quad (1)$$

$$T_B \leq T \leq T_C: \quad S_e(T) = a_g \cdot S_T \cdot S \cdot \eta \cdot 2.5 \quad (2)$$

$$T_C \leq T \leq T_D: \quad S_e(T) = a_g \cdot S_T \cdot S \cdot \eta \cdot 2.5 \cdot \frac{T_C}{T} \quad (3)$$

$$T_D \leq T \leq 4s: \quad S_e(T) = a_g \cdot S_T \cdot S \cdot \eta \cdot 2.5 \cdot \frac{T_C T_D}{T^2} \quad (4)$$

where:

- $S_e(T)$ is the elastic response spectrum;
- T is the vibration period of a linear single-degree-of-freedom system;
- a_g is the design ground acceleration type A ground ($a_g = \gamma_I a_{gr}$);
- a_{gr} is the reference peak ground acceleration on type A ground
- γ_I is the importance factor
- T_B is the lower limit of the period of the constant acceleration branch;
- T_C is the upper limit of the period of the constant acceleration branch;
- T_D is the value defining the beginning of the constant displacement response range of the spectrum;
- S is the soil factor
- S_T is the topographic amplification factor
- η is the damping correction factor with a reference value of $\eta = 1$ for 5% viscous damping;

The values of the periods T_B , T_C , T_D and of the soil factor S that describes the shape of the elastic response spectra depend upon the ground type. For the aforementioned parameters and the soil classification, the reader may refer to Chapter 3 of the EC8. The seismic survey report (which Seed Consulting provided) found a value of $v_{s,30}$ greater than 800m/s that classifies the construction site as type A ground.

In Table 1.8 are given the value of parameters to construct the horizontal response spectra according to the recommendations of the EC8. We refer to those parameters as the national annex to provide these values is missing. The values of reference ground accelerations, a_{gr} , computed from the PSHA analyses for different return periods are presented in Table 1.9.

Table 1.8 Recommended values of parameters describing the horizontal elastic response spectra (EC8)

$V_{s,30}$ (m/s)	Ground	Spectrum	T_B	T_C	T_D	S	S_T
------------------	--------	----------	-------	-------	-------	-----	-------

	Type	Type					
≥ 800	A	Type 1	0.15	0.4	2	1	1.1
≥ 800	A	Type 2	0.05	0.25	1.2	1	1.1

Table 1.9: Reference ground acceleration computed from the PSHA analysis presented in Chapter 4

Return Period, T_{NCR} [years]	a_{gr} [g]
95	0.260
475	0.404
2,450	0.654
10,000	0.910

The two following figures depict the comparison between the EC8 spectra types and the uniform hazard spectra. It can be observed that the EC8-Type 1 spectra give higher spectral values in the long period range as compared to the values of the uniform hazard spectra computed from the PSHA procedure. Conversely, the EC8-Type 2 spectra envelop better the uniform hazard spectra in the low range of periods. Based on these discrepancies and to be in the favour of a more conservative design, we do suggest the designers to select the EC8 response spectra type based on the significant vibration periods of the structures to be designed. Appreciating the above consideration, we select the ground motion time histories that are spectrum-compatible with both the EC8-Type 1 and -Type 2 spectra.

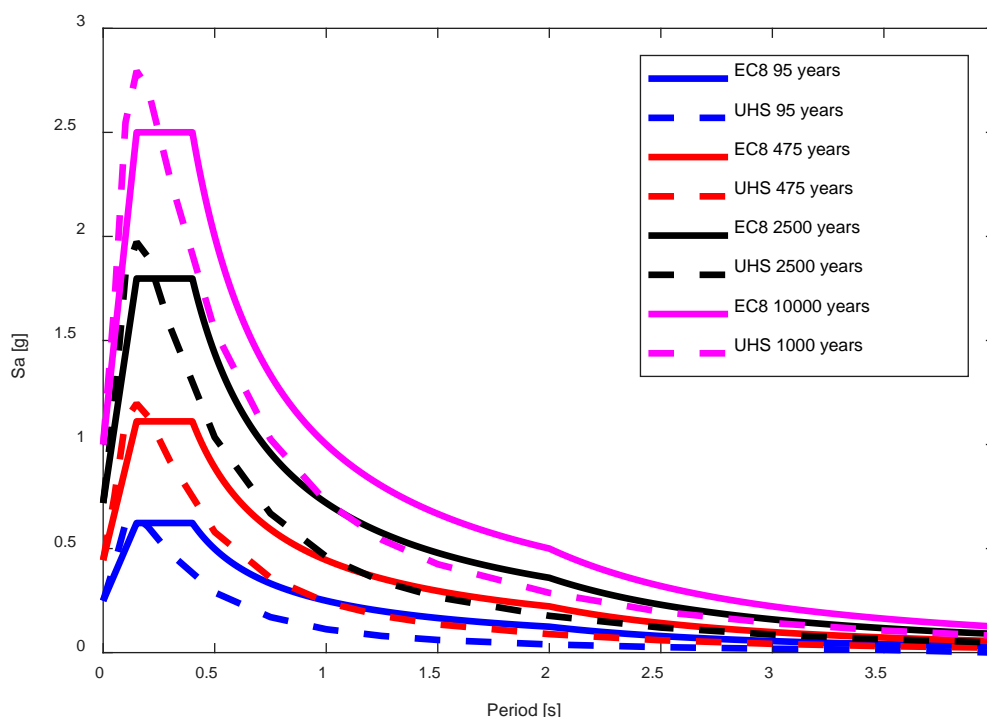


Figure 1.14 UHS and EC8-Type 1 spectra for different return periods.

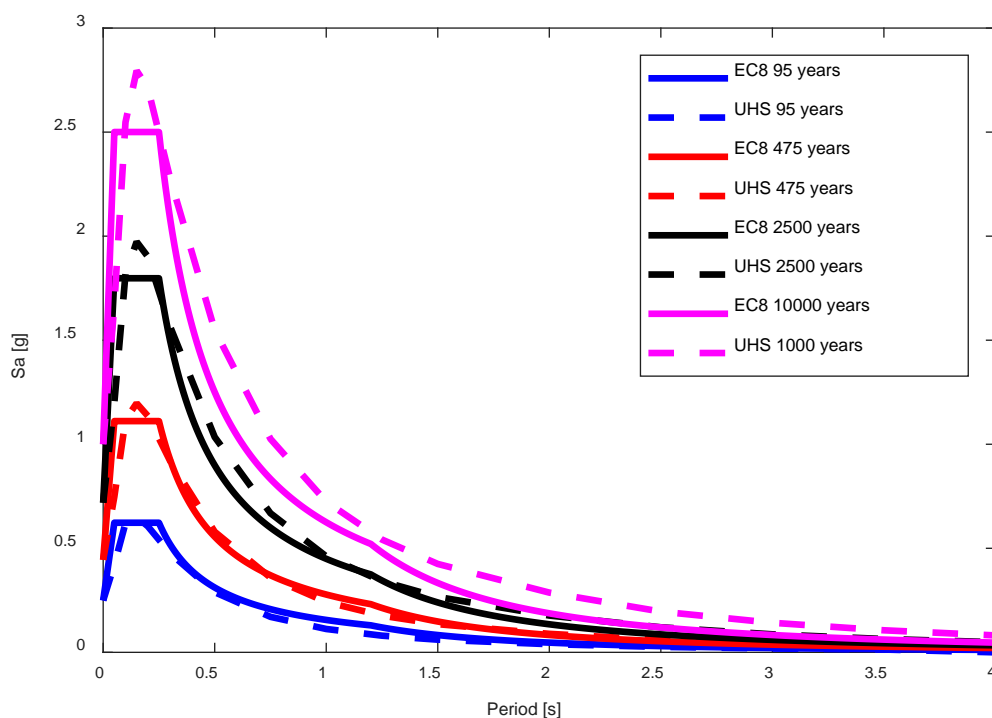


Figure 1.15 UHS and EC8-Type 2 spectra for different return periods.

1.6.2 Vertical Elastic Spectra

The vertical elastic spectra according to Eurocode 8 are defined based on the following expressions:

$$0 \leq T \leq T_B: \quad S_{ve}(T) = a_{vg} \cdot S_T \cdot \left[1 + \frac{T}{T_B} \cdot (\eta \cdot 3.0 - 1) \right] \quad (5)$$

$$T_B \leq T \leq T_C: \quad S_{ve}(T) = a_{vg} \cdot S_T \cdot \eta \cdot 3.0 \quad (6)$$

$$T_C \leq T \leq T_D: \quad S_{ve}(T) = a_{vg} \cdot S_T \cdot \eta \cdot 3.0 \cdot \frac{T_C}{T} \quad (7)$$

$$T_D \leq T \leq 4s: \quad S_{ve}(T) = a_{vg} \cdot S_T \cdot \eta \cdot 3.0 \cdot \frac{T_C T_D}{T^2} \quad (8)$$

In the absence of the national annex, we suggest that the values of T_B , T_C , T_D , and a_{vg} for defining the vertical spectra to be obtained from the recommended values of the EC8 for the spectra of Type 1, Table 1.10. In favour of avoiding human errors, we suggest to the user that the parameters presented herein from the different parts of EC8 be retrieved directly from the relevant part of the codes.

Table 1.10 Recommended values of parameters describing the vertical elastic response spectra (excerpt from EC8)

Spectrum type	a_{vg}/a_g	T_B	T_C	T_D
Type 1	0.9	0.05	0.15	1
Type 2	0.45	0.05	0.15	1

1.6.3 Ground Motion Time Histories compatible with EC8 Part 2 requirements

Based on section 3.2.3 of EC8 Part 2, the following provisions apply to the ground motions time-histories:

1. When a non-linear time-history analysis is carried out, at least three pairs of horizontal ground motion time-history components shall be used. The pairs should be selected from recorded events with magnitudes, source distances, and mechanisms consistent with those that define the design seismic action
2. When the required number of pairs of appropriate recorded ground motions is not available, appropriate modified recordings or simulated accelerograms may replace the missing recorded motions.
3. Consistency to the relevant 5% damped elastic response spectrum of the design seismic action shall be established by scaling the amplitude of motions as follows.
 - a. For each earthquake consisting of a pair of horizontal motions, the SRSS spectrum shall be established by taking the square root of the sum of squares of the damped spectra of each component.
 - b. The spectrum of the ensemble of earthquakes shall be formed by taking the average value of the SRSS spectra of the individual earthquakes of the previous step.
 - c. The ensemble spectrum shall be scaled so that it is not lower than 1,3 times the 5%- damped elastic response spectrum of the design seismic action, in the period range between $0,2 T_1$ and $1,5 T_1$, where T_1 is the natural period of the fundamental mode of the structure in the case of a ductile bridge, or the effective period (T_{en}) of the isolation system in the case of a bridge with seismic isolation.
 - d. The scaling factor derived from the previous step shall be applied to all individual seismic motion components.
4. When the SRSS spectrum of the components of a recorded accelerogram accelerations the ratio of which to the corresponding values of the elastic response spectrum of the design seismic action shows large variation in the period range in (3)Pc, modification of the recorded accelerogram may be carried out, so that the SRSS spectrum of the modified components is in closer agreement with the elastic response spectrum of the design seismic action.
5. The components of each pair of time-histories shall be applied simultaneously.
6. When three component ground motion time-history recordings are used for nonlinear time-history analysis, scaling of the horizontal pairs of components may be carried out in accordance with (3)P, independently from the scaling of the vertical components. The latter shall be effected so that the average of the relevant spectra of the ensemble is not lower by more than 10 % of the 5% damped elastic response spectrum of the vertical design seismic action in the period range between $0,2 T_v$ and $1,5 T_v$, where T_v is the period of the lowest mode where the response to the vertical component prevails over the response to the horizontal components (e.g., in terms of participating mass).
7. The use of pairs of horizontal ground motion recordings in combination with vertical recordings of different seismic motions, consistent with the requirements of (1)P above, is also allowed. The independent scaling of the pairs of horizontal recordings and of the vertical recordings shall be carried out as in (6).
8. Modification of the recorded vertical component in (6) and (7) is permitted using the method specified in (4).

1.6.4 Selected records and discussion

Based on the recommendations of EC8-part 2 discussed above, sets of records for horizontal and vertical records are selected. Herein, the records are selected for both Type 1 and Type 2 design spectrum of EC8 and we leave the designer to select the best that believes fit with the conditions of the site. However, should the long periods of vibrations be of the interest, the authors of this report suggest a preference for Type 1 sets because they are essentially more conservative in the long period range. The records are selected from the NGA-West ground motion database (Chiou et al. 2008). To maintain the consistency of the site soil class with the selected records, only records with $V_{s30} \geq 600$ m/s are selected. In each set, seven records are selected such

that the spectrum obtained from the ensemble of records in the period range of interest (herein assumed [0.2, 1.5] s) is above the target. The selection for the horizontal components is based on the geometric mean of the two components and the scaling factor is limited to maximum 3.0. The properties of the selected records are listed in Table 1.11, Table 1.12, Table 1.13 and Table 1.14 and the quality of the fit of the spectra are shown in Figure 1.16, Figure 1.17, Figure 1.18 and Figure 1.19.

Table 1.11 Horizontal ground motion records selected corresponding with the EC8-Type 1 design spectrum

Sequence Number					Epicentral		Scale Factor
No.	NGA-W	Earthquake Name	Date	Magnitude	Distance [km]	V _{s30} [m/s]	
1	150	COYOTE LAKE	08/06/1979	5.7	4.4	663	2.45
2	585	BAJA CALIF	02/07/1987	5.5	3.7	660	1.43
3	126	GAZLI	05/17/1976	6.8	12.8	660	1.38
4	495	NAHANNI	12/23/1985	6.8	6.8	660	2.06
5	300	IRPINIA	11/23/1980	6.2	12.0	600	2.85
6	1012	NORTHRIDGE	01/17/1994	6.7	14.4	706	2.71
7	1111	KOBE	01/16/1995	6.9	8.7	609	1.78

Table 1.12 Vertical ground motion records selected corresponding with the EC8-Type 1 design spectrum

Sequence Number					Epicentral		Scale Factor
No.	NGA-W	Earthquake Name	Date	Magnitude	Distance [km]	V _{s30} [m/s]	
1	585	BAJA CALIF	02/07/1987	5.5	3.7	660	1.12
2	459	MORGAN HILL	04/24/1984	6.2	36.3	663	1.76
3	126	GAZLI	05/17/1976	6.8	12.8	660	0.44
4	765	LOMA PRIETA	10/18/1989	6.9	28.6	1428	2.15
5	495	NAHANN	12/23/1985	6.8	6.8	660	0.64
6	994	NORTHRIDGE	01/17/1994	6.7	25.4	1016	2.41
7	1161	KOCAELI	08/17/1999	7.5	47.0	792	2.48

Table 1.13 Horizontal ground motion records selected corresponding with the EC8-Type 2 design spectrum

Sequence Number					Epicentral		Scale Factor
No.	NGA-W	Earthquake Name	Date	Magnitude	Distance [km]	V _{s30} [m/s]	
1	1078	NORTHRIDGE	01/17/1994	6.7	14.7	715	2.40
2	1596	CHI-CHI	09/20/1999	7.6	14.2	664	1.09
3	1549	CHI-CHI	09/20/1999	7.6	14.2	664	1.01
4	495	NAHANNI	12/23/1985	6.8	6.8	660	1.26
5	1111	KOBE	01/16/1995	6.9	8.7	609	1.09
6	1012	NORTHRIDGE	01/17/1994	6.7	14.4	706	1.66
7	1165	KOCAELI	08/17/1999	7.5	5.3	811	2.16

Table 1.14 Vertical ground motion records selected corresponding with the EC8-Type 2 design spectrum

No.	Sequence Number	Earthquake Name	Date	Magnitude	Epicentral Distance [km]	V_{s30} [m/s]	Scale Factor
1	1159	KOCAELI	08/17/1999	7.51	187.0	660	3.00
2	585	BAJA CALIF	02/07/1987	5.50	3.7	660	0.56
3	222	LIVERMORE	01/27/1980	5.42	10.3	713	2.43
4	414	COALINGA	07/22/1983	5.77	13.4	617	2.53
5	495	NAHANN	12/23/1985	6.76	6.8	660	0.32
6	126	GAZLI	05/17/1976	6.80	12.8	660	0.22
7	459	MORGAN HILL	04/24/1984	6.19	36.3	663	0.88

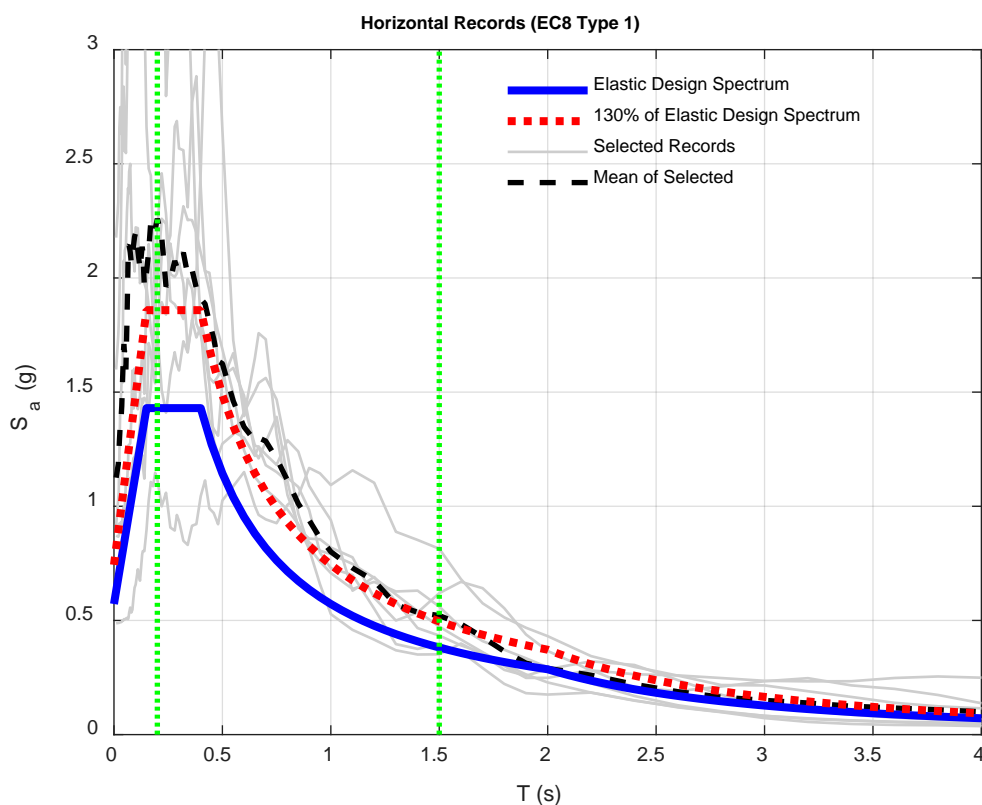


Figure 1.16 Horizontal ground motion records selected corresponding with the EC8-Type 1 design spectrum

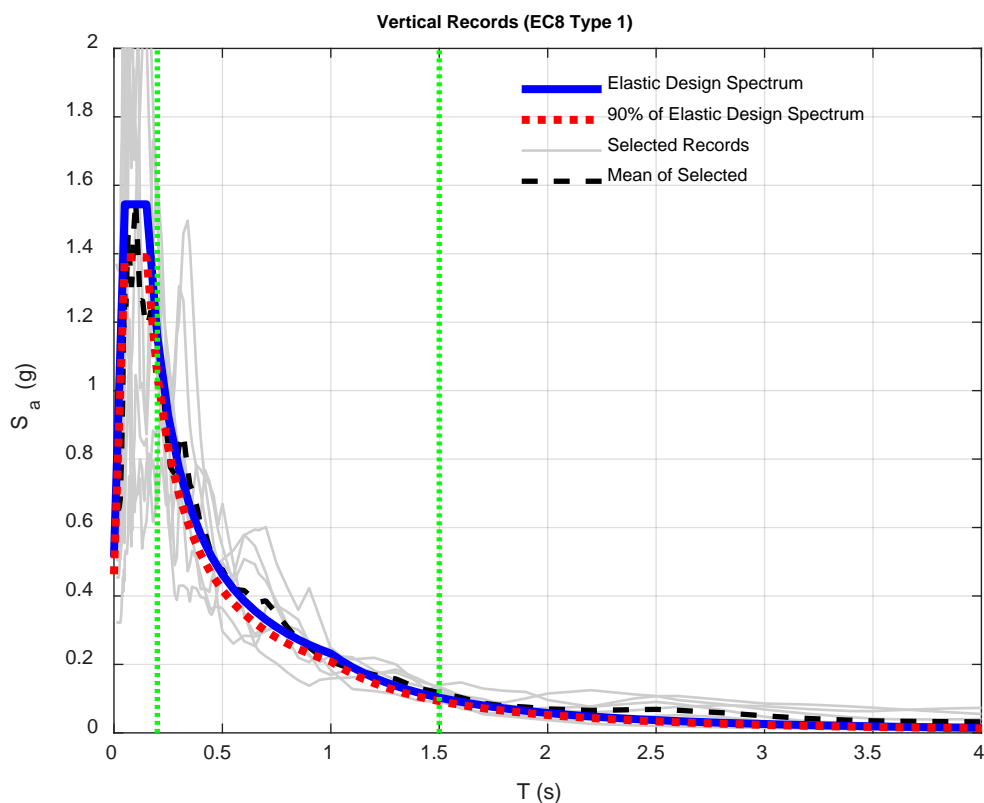


Figure 1.17 Vertical ground motion records selected corresponding with the EC8-Type 1 design spectrum

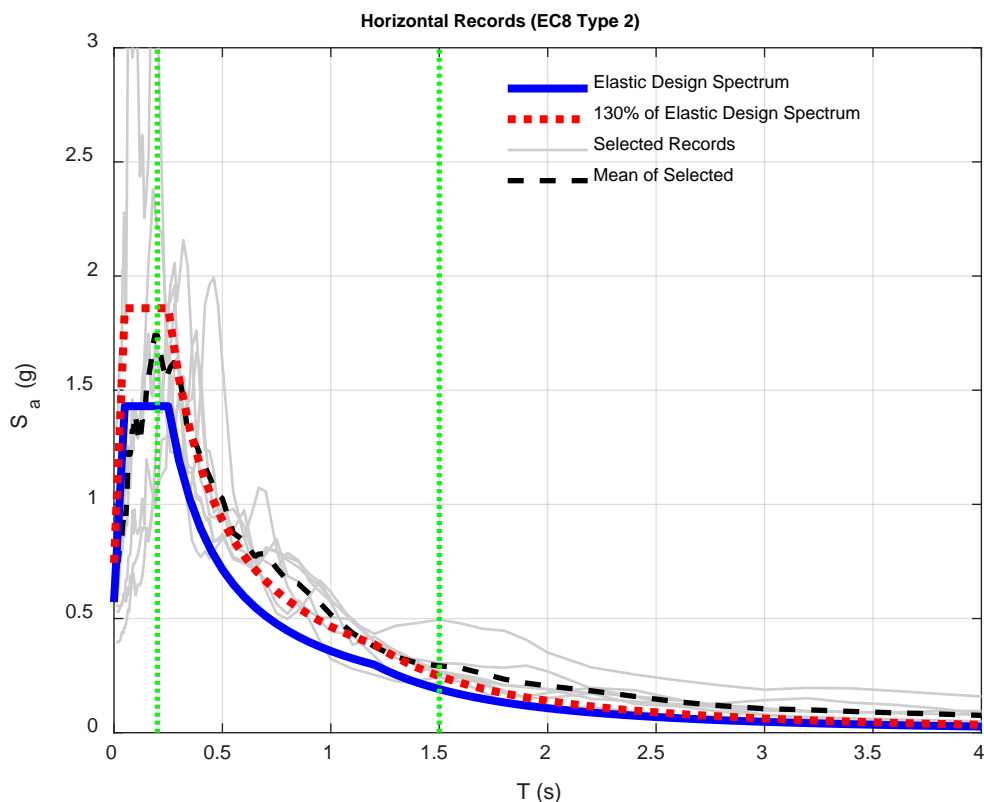


Figure 1.18 Horizontal ground motion records selected corresponding with the EC8-Type 2 design spectrum

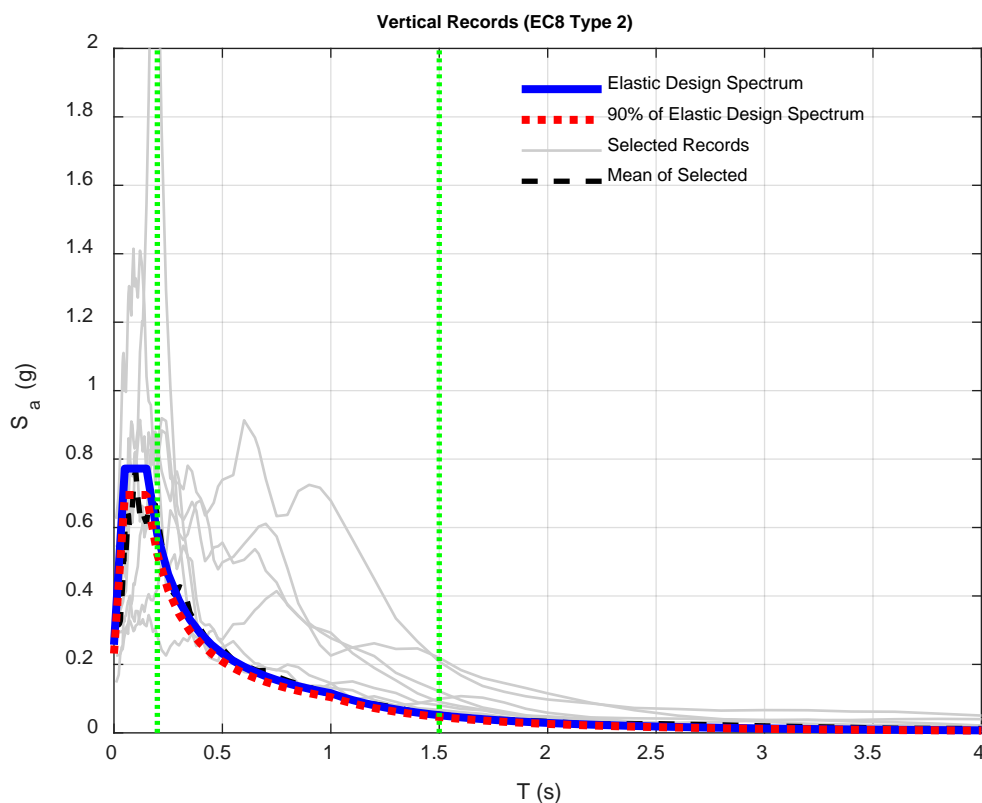


Figure 1.19 Vertical ground motion records selected corresponding with the EC8-Type 2 design spectrum

1.7 Analysis of the actual in force Albanian design code in respect to seismic action and comparisons with the requirements of EC8.

Based on the seismic intensity map of the KTP N.2 89, Figure 1.20, and the Albania geologic map¹, the tunnel site area is prone to a seismic intensity VIII on the MSK-64 scale and is located on a soil category I. The seismic coefficient k_E , the ratio of PGA to gravitational acceleration, according to KTP-N.2-89 is 0.16, Table 1.15.

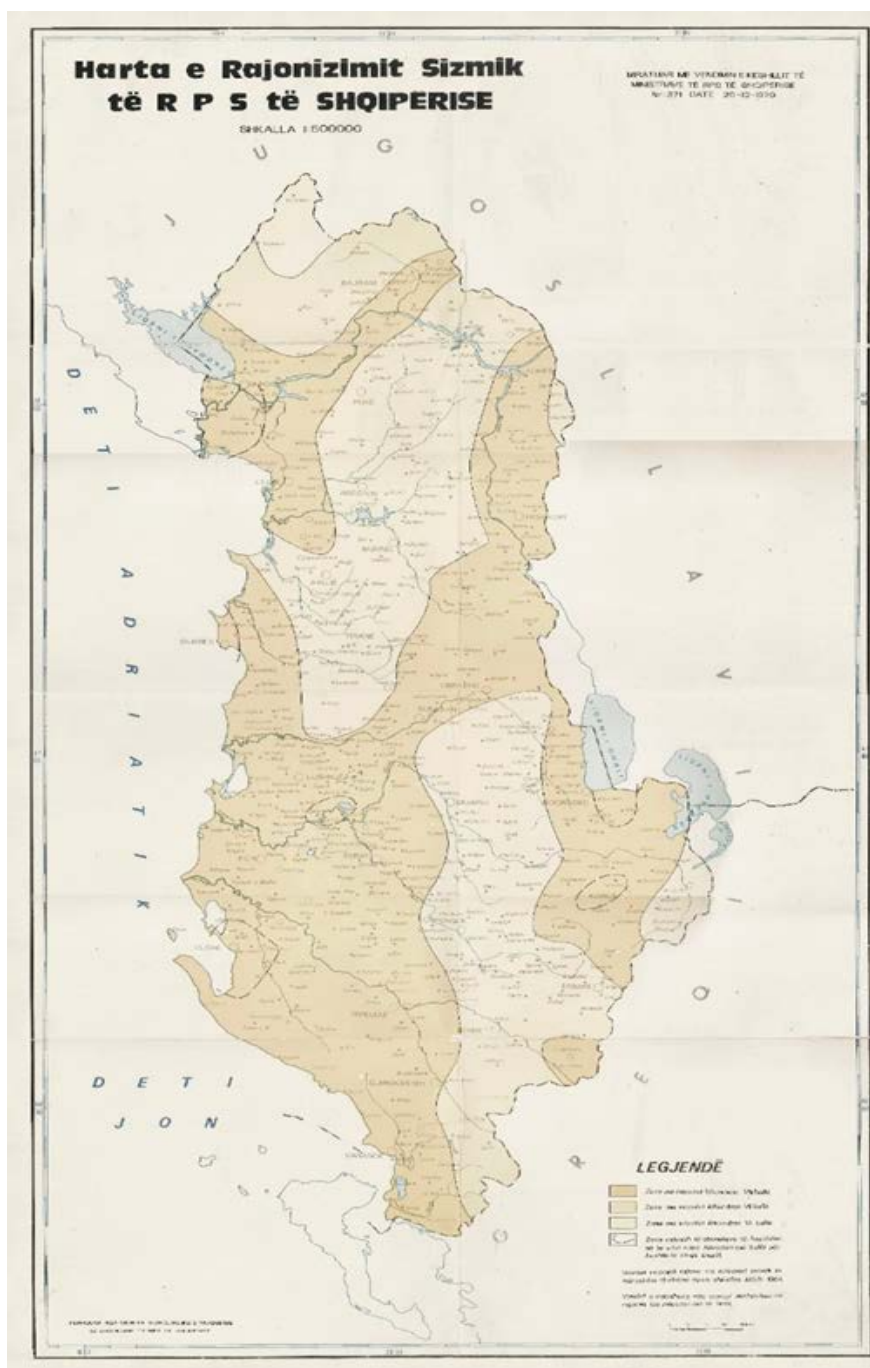


Figure 1.20 Seismic hazard map in KTP-N2-89, in MSK-64 macroseismic intensity scale

¹ https://geoportal.asig.gov.al/map/?fc_name=harta_gjeologjike_100k&auto=true

Table 1.15 Seismic coefficients according to KTP-N.2-89

Soil category	Intensity VII	Intensity VIII	Intensity IX
I	0.08	0.16	0.27
II	0.11	0.22	0.36
III	0.14	0.26	0.42

The elastic horizontal response spectrum is defined based on the following formula:

$$S_{ah}(T) = k_E k_r \beta g \quad (9)$$

where:

k_E , is the coefficient of seismicity. The coefficient represents the ratio of the peak ground acceleration to the gravitational acceleration;

g , is the gravitational acceleration;

k_r , is the building importance factor, *e.g.*, for ordinary buildings is equal to 1, for buildings that are important for post-earthquake recovery is 1.5, for buildings whose damage may cause serious consequences to the life safety of its occupants for *e.g.* schools, theatres, etc. is 1.3, etc;

β , is the dynamic factor that accounts for the effect of dynamic properties of the structure on the design spectral acceleration and is function of the period of structure, T , and the soil category, Table 1.16.

Table 1.16: Dynamic factor β , according to KTP-N.2-89

Category I – rock	Category II – weathered rock, stiff and medium soil	Category III – soft soil
$0.65 \leq \beta = \frac{0.7}{T} \leq 2.3$	$0.65 \leq \beta = \frac{0.8}{T} \leq 2$	$0.65 \leq \beta = \frac{1.1}{T} \leq 1.7$

In Figure 1.21 is presented a comparison between the elastic spectra based on the KTP N.2-89 and EC8 code. The importance coefficients are assumed equal to 1. One can notice that for the range of periods 0 to around 2.7 sec the EC8 spectral demand is drastically higher than the spectral demanded required from the national code KTP N.2-89.

The elastic vertical response spectrum for bridge designs is defined based on the following formula:

$$S_{va}(T) = 0.5 k_E k_r \beta g \quad (10)$$

A comparison of the vertical response spectrum based on KTP N.2-89 and the vertical spectrum according to EC8 is presented in Figure 1.22. The difference between the two spectra in the range of periods 0 to around 1.6s is significant.

Since the design spectra values are subjected to changes due to different parameters, like the importance factor of different construction works, etc., we leave the full comparison between the two codes and the decision on which code to adopt for the design to the designer.

We restate here that in favour of avoiding human errors, we suggest to the users of the report that the parameters presented herein from the different sections of the KTP N.2-89 to be directly retrieved from the relevant part of the code.

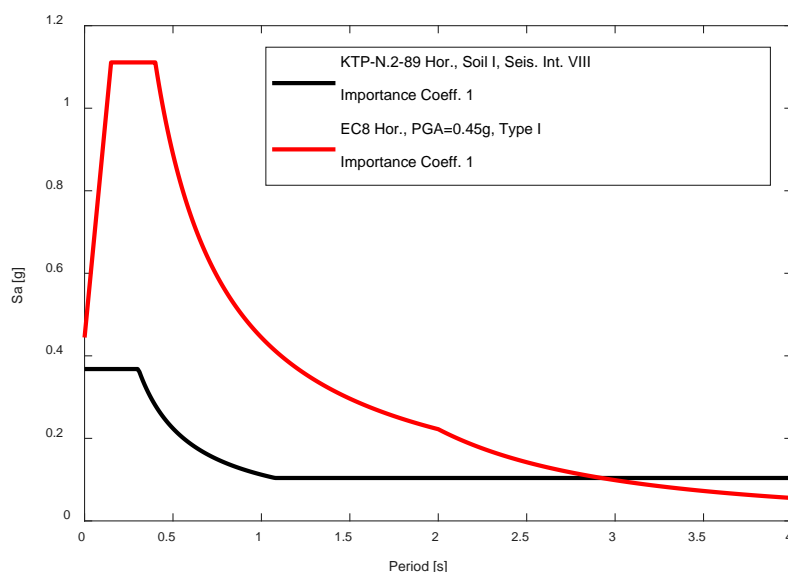


Figure 1.21 Comparison of the horizontal elastic spectra according to KTP N.2 89 and EC8

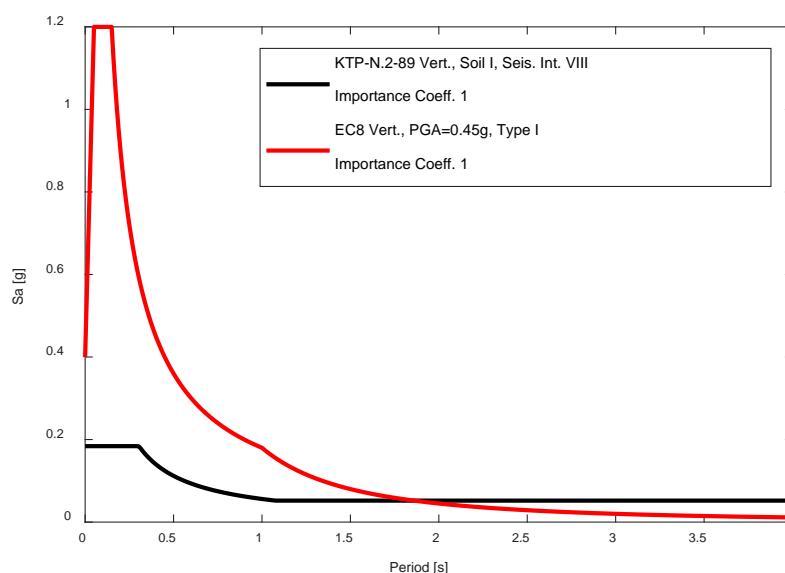


Figure 1.22 Comparison of the vertical elastic spectra according to KTP N.2 89 and EC8

1.8 Conclusion and Recommendations

In this report, we present the PSHA and DSHA analyses conducted to assess the seismic hazard of the tunnel site area. We provided the estimates of the peak ground accelerations and spectral acceleration values for different return periods and constructed the UHS for four return periods. We provided the hazard curves, *i.e.*, the curve that gives the probability of exceedance a particular value y^* in a given time window, of each spectral acceleration point of the UHS. Besides, a Determinist Seismic Hazard Assessment was carried out to assess the peak ground accelerations that can be generated by the two closest seismogenic faults. Since the tunnel site area is located in a mountain region, we computed the topographic amplification factor in agreement with the EC8 procedure. It is suggested that the minimum topographic factor that can be applied following the EC8 requirement is 1.1. Two sets of seven 3D accelerograms that are compatible with the EC8 type 1 and type 2 target spectra are selected and provided. Finally, a short presentation of the elastic spectra computed in line with Albania's current seismic code is presented.

1.9 Deliverables

Table 1.17 Table of deliverables of this study

No.	Name of the file	Description
1	Final_Report.pdf	The final report file in pdf that provides a description about the methodology and the results.
2	Outputs.xlsx	<p>This excel file provides the outputs of the study in different specific sheets as follows:</p> <ol style="list-style-type: none"> 1- Hazard-Curves: the full hazard curves for different spectral ordinates. 2- UHS: the Uniform hazard spectra for 95, 475, 2475 and 10000 years return periods. 3- Deterministic_Spectrum: the mean and standard deviation of the response spectra for the two selected scenarios are listed. 4- Deterministic_Ds5-95: the results of the duration analysis. 5- Records_Type1: Table of the properties of the selected records for Design spectrum Type 1 together with the as-recorded (with no scaling) response spectra of the two horizontal and vertical components 6- Records_Type2: Table of the properties of the selected records for Design spectrum Type 2 together with the as-recorded (with no scaling) response spectra of the two horizontal and vertical components
4	Records.rar	<p>This folder contains the acceleration time-histories of the selected ground motions in two-column format. It contains two subfolders named Horizontal and Vertical. In each Folder, there are two subfolders named Type1 and Type2. For Horizontal records for each selected record two components are provided (total 7×2=14 files), while for the vertical records 7 files are stored in the corresponding folder. Note that the records in these folders are not scaled and thus when using them the user should multiply the acceleration time histories with the provided scaling factors. The name of each record is listed in the Outputs.xlsx file in sheets Records_Type1 and Records_Type2 in columns I and J.</p>

1.10 References

Afshari K, Stewart JP (2016) Physically Parameterized Prediction Equations for Significant Duration in Active Crustal Regions Earthquake Spectra 32:2057-2081 doi:10.1193/063015eqs106m

- Akkar S, Sandikkaya MA, Bommer JJ (2014) Empirical ground-motion models for point- and extended-source crustal earthquake scenarios in Europe and the Middle East *Bulletin of Earthquake Engineering* 12:359-387 doi:10.1007/s10518-013-9461-4
- Aliaj, SH., Koçiu, S., Muço, B., Sulstarova, E., 2010, "Seismicity, Seismotectonics and Probabilistic Seismic Hazard of Albania, Science Academy", Tirana, Albania.
- Baker J, Cornell C (2006) Spectral shape, epsilon and record selection *Earthquake engineering and structural dynamics* 35:1077–109
- Basili R., Kastelic V., Demircioglu M. B., Garcia Moreno D., Nemser E. S., Petricca P., Sboras S. P., Besana-Ostman G. M., Cabral J., Camelbeeck T., Caputo R., Danciu L., Domac H., Fonseca J., García-Mayordomo J., Giardini D., Glavatovic B., Gulen L., Ince Y., Pavlides S., Sesetyan K., Tarabusi G., Tiberti M. M., Utkucu M., Valensise G., Vanneste K., Vilanova S., Wössner J. (2013). The European Database of Seismogenic Faults (EDSF) compiled in the framework of the Project SHARE. <http://diss.rm.ingv.it/share-edsf/>, doi: 10.6092/INGV.IT-SHARE-EDSF.
- Bindi D, Massa M, Luzi L, Ameri G, Pacor F, Puglia R, Augliera P (2014) Pan-European ground-motion prediction equations for the average horizontal component of PGA, PGV, and 5 %-damped PSA at spectral periods up to 3.0 s using the RESORCE dataset *Bulletin of Earthquake Engineering* 12:391-430 doi:10.1007/s10518-013-9525-5
- Boore DM, Stewart JP, Seyhan E, Atkinson GM (2014) NGA-West2 Equations for Predicting PGA, PGV, and 5% Damped PSA for Shallow Crustal Earthquakes *Earthquake Spectra* 30:1057-1085 doi:10.1193/070113eqs184m
- Chiou B, Darragh R, Gregor N, Silva W (2008) NGA Project Strong-Motion Database *Earthquake Spectra* 24:23-44 doi:10.1193/1.2894831
- EN 1998-1, 2005, "Eurocode 8: Design of structures for earthquake resistance. Part 1: General rules, seismic actions, and rules for buildings," CEN
- EN 1998-2, 2005, "Eurocode 8: Design of structures for earthquake resistance. Part 2: Bridges," CEN
- EN 1998-5, 2005, "Eurocode 8: Design of structures for earthquake resistance. Part 5: Foundations, retaining structures, and geotechnical aspects," CEN
- Chiou BS-J, Youngs RR (2014) Update of the Chiou and Youngs NGA Model for the Average Horizontal Component of Peak Ground Motion and Response Spectra *Earthquake Spectra* 30:1117-1153 doi:10.1193/072813eqs219m
- Duni L, Kuka N, Kuka S, Fundo A (2010) Towards a New Seismic Hazard Assessment of Albania Paper presented at the 14ECEE,
- Gulerce Z et al. (2017) SEISMIC HAZARD MAPS FOR THE WESTERN BALKAN KARTE POTRESNE OPASNOSTI ZA PODRUČJE ZAPADNOG BALKANA *Inženjerstvo okoliša* 4:7-17
- Kijko A (2004) Estimation of the Maximum Earthquake Magnitude, m_{max} *Pure and Applied Geophysics* 161:1655-1681 doi:10.1007/s00024-004-2531-4
- KTP-N.2-89, 1989, "Technical Aseismic Regulations," Publication of Academy of Sciences and Ministry of Constructions, Tirana, Albania. (in Albanian)
- Mihaljević J et al. (2017) BSHAP seismic source characterization models for the Western Balkan region *Bulletin of Earthquake Engineering* 15:3963-3985 doi:10.1007/s10518-017-0143-5
- Muco B, Kiratzi A, Sulstarova E, Kociu S, Peci V, Scordilis E (2002) Probabilistic Seismic Hazard assessment in Albania AGU Fall Meeting Abstracts
- Pagani M et al. (2014) OpenQuake Engine: an Open Hazard (and Risk) Software for the Global Earthquake Model *Seismol Res Lett* 85:692–702
- Pagliaroli A, Lanzo G, D'Elia B, Costanzo A, Silvestri F (2007) Topographic amplification factor associated to cliff morphology: numerical results from two case studies in Southern Italy and comparison with EC8 recommendations. XIV European Conference on Soil Mechanics and Geotechnical Engineering, Workshop on geotechnical aspects of EC8, Madrid, Spain.
- Weichert DH (1980) Estimation of the earthquake recurrence parameters for unequal observation periods for different magnitudes *Bulletin of the Seismological Society of America* 70:1337-1346